Eosinophilic, solid, and cystic renal cell carcinoma

Eosinophilic, Solid And Cystic Renal Cell Carcinoma With Frequent Cytokeratin 20 Reactivity: Clinicopathologic Study of 16 Unique Neoplasms Occurring Predominantly in Women

Kiril Trpkov MD[1], Ondrej Hes MD, PhD[2], Michael Bonert MD[1], Jose I Lopez MD, PhD[3], Stephen Bonsib MD[4], Gabriella Nesi MD[5], Eva Comperat MD[6], Mathilde Sibony MD[7], Daniel M Berney MD[8], Petr Martinek MSc[2], Stela Bulimbasic MD[9], Saul Suster MD[10], Ankur Sangoi MD[11], Asli Yilmaz MD[1], Ming Zhou MD, PhD [12], Cristina Magi-Galluzzi MD, PhD [13], and Jesse K McKenney MD[13]

[1]Calgary Laboratory Services and University of Calgary, Calgary, AB, Canada; [2]Charles University, Pilsen, Czech Republic; [3]Cruces University Hospital, BioCruces Institute, University of the Basque Country (UPV/EHU), Barakaldo, Bizkaia, Spain; [4]Nephropath, Little Rock, AR, United States; [5]Carregi Hospital, Florence, Italy; [6]Pitié-Salpêtrière Hospital, Paris, France; [7]Hopital Cochin, Paris, France; [8]Barts Cancer Institute, Queen Mary University of London, London, United Kingdom; [9]University Hospital Dubrava, Zagreb, Croatia; [10]Medical College Wisconsin, Milwaukee, WI; [11]El Camino Hospital, Mountain View, CA [12]New York University Medical Center, New York, NY and [13]Robert J. Tomsich Pathology and Laboratory Medicine Institute, Cleveland Clinic, Cleveland, OH.

Correspondence:

Kiril Trpkov, MD, FRCPC, Department of Pathology and Laboratory Medicine, Calgary Laboratory Services and University of Calgary, Rockyview General Hospital, 7007 14 Street, Calgary, AB, Canada, T2V 1P9; Email: kiril.trpkov@cls.ab.ca; Tel: (403)9433443; Fax: (403)9433333;

Funding disclosures and conflicts of interest:

Study was supported in part by Calgary Laboratory Services, by Charles University Research Fund (project number P36) and by the project CZ.1.05/2.1.00/03.0076 from the European Regional Development Fund. OncoScan™ molecular karyotyping was supported by Affymetrix, Inc. and was performed at ARUP Laboratories.

Authors have no other funding disclosures or conflicts of interest to report.

Abstract

A unique renal neoplasm characterized by eosinophilic cytoplasm and solid and cystic growth was recently reported in patients with Tuberosus Sclerosis Complex (TSC). We searched multiple institutional archives and consult files in an attempt to identify a sporadic counterpart. We identified 16 morphologically identical cases, all in females, without clinical features of TSC. The median age was 57 years (range 31-75 y). Tumors were yellow-gray and had a solid and cystic (12) or only solid appearance (4). Average tumor size was 50 mm (median, 38.5 mm; range 15-135 mm). Microscopically, the tumors showed solid areas admixed with variably sized macro and microcysts. The cells had voluminous eosinophilic cytoplasm with frequent cytoplasmic stippling and round to oval nuclei with prominent nucleoli (ISUP nucleolar grade 3). Scattered histiocytes and lymphocytes were invariably present. Thirteen of 16 patients were stage pT1; 2 were pT2, and 1 was pT3a. The cells demonstrated a distinct immunoprofile: nuclear PAX-8, diffuse (or focal) cytokeratin 20, patchy AMACR, but only rare focal cytokeratin 7 or CD117 reactivity. Thirteen of 14 patients with follow-up were alive and without disease progression after 2 to 138 months (mean: 53 mo; median: 37.5 mo); 1 patient died of other causes. We propose that "eosinophilic, solid and cystic renal cell carcinoma", which occurs predominantly in females and is characterized by distinct morphologic features, frequent cytokeratin 20 reactivity and indolent behaviour, represents a novel unrecognized subtype of renal cell carcinoma, which can be found associated with TSC, but also may occur sporadically.

Running title: Eosinophilic Solid and Cystic Renal Cell Carcinoma

Key words: Eosinophilic tumor; renal cell carcinoma; tuberous sclerosis; CK20; unclassified oncocytic tumor; unclassified renal cell carcinoma

Introduction

Recent studies have documented a unique type of renal neoplasm exhibiting eosinophilic cytoplasm and varying solid and cystic architectural growth, found predominantly in female patients with Tuberous Sclerosis Complex (TSC).(1, 2) In contrast to the other patterns of renal cell carcinoma encountered in association with TSC, which were originally described in a sporadic setting (i.e. chromophobe-like and renal cell carcinoma with smooth muscle stroma), to our knowledge, these unique eosinophilic and cystic neoplasms have not been previously recognized or documented, other than in association with TSC. They are currently not included, or recognized as a provisional entity, in the 2013 International Society of Urological Pathology (ISUP) Vancouver Classification of renal tumors.(3)

Although these neoplasms seem to demonstrate unique morphologic, clinical and immunohistochemical features, they have most likely been historically signed-out in routine diagnostic practice as "unclassified renal cell carcinoma" or descriptively designated "unclassified renal neoplasm (or carcinoma) with oncocytic or eosinophilic morphology" (or some combination of these descriptive terms).

After encountering histologically identical neoplasms in a clinically sporadic setting, we initiated an international collaboration to identify and study a larger series of these unique renal tumors. Our aim was to establish and characterize their clinical and morphologic features, immunohistochemical profile, ultrastructural features, and to determine their clinical behaviour and prognosis. We also performed a molecular karyotypic analysis and array comparative

genomic hybridization in a limited number of cases, to evaluate for possible recurring genomic alterations.

Material and Methods

An institutional Ethics Review was obtained for this study.

Pathology evaluation

We searched for renal neoplasms labelled in the initial sign-out as "unclassifed, oncocytic or eosinophilic" in multiple institutional archives and consult files of surgical pathologists with subspecialty interest in urologic pathology. Many of participating institutions represent centers with large in-house and consult uropathology practices. All cases were reviewed by two urologic pathologists, comparing the features with the index cases. One or multiple haematoxylin and eosin slides were available for review in all cases. Clinicopathologic and follow-up data were collected by review of the institutional records and by contacting the consulting pathologists.

Immunochemical studies were carried out using a panel of primary antibodies, commonly used in urologic pathology, which included: PAX8, AMACR, CD10, CD117 (C-kit), EMA, CK7, CK20, CA9, AE1/AE3, CK8/18, and vimentin. The immunohistochemistry evaluation for 14 cases was performed in 2 laboratories on representative blocks provided by the originating pathologist, and was read by two pathologists (KT, JMK). The immunohistochemistry and the evaluation of 2 additional cases was done by one pathologist in a separate laboratory (JIL). The immunostains for Hamartin and Tuberin were performed in one laboratory on the available unstained slides and were interpreted by one pathologist (SB). 'Negative' IHC result was

considered if less than 5% of cells stained; 'focal' was if 5-25% cells were reactive, and 'positive' was if >25% of cells were reactive.

Electron microscopy evaluation was performed on two cases. Small pieces of formalin fixed paraffin embedded (FFPE) from cases #9 and #15 were deparaffinized and further routinely processed for ultrastructural analysis. Semithin sections of epoxy embedded tissue were stained with toluidine blue, and examined by light microscopy. Ultrathin sections from representative area were cut, stained with uranyl acetate and lead citrate, and examined with a Jeol (Tokyo, Japan) JEM 1400 Transmission Electronic Microscope.

Molecular karyotyping

Molecular karyotyping was performed from FFPE tissue blocks in 3 cases (#2, #8 and #13). Eight sections, each 10 µm thick, were obtained of the FFPE tissue blocks. DNA was extracted and purified using the Ambion Recover All Total Nucleic Acid Isolation kit (Applied Biosystems, Carlsbad, California) following the manufacturer's protocol. Briefly, the procedure entails deparaffinization with xylene, protease digestion, ethanol, and filter cartridge– based DNA isolation lowed by an on-filter RNase treatment and elution. Extracted DNA was quantified using Quant-iT PicoGreen ds DNA HS reagent and Qubit fluorometer (Invitrogen, Carlsbad, CA) following the manufacturer's procedure. OncoScan Assay Kit Ver 3.0 was performed according to the manufacturer's procedure. Briefly, the assay uses molecular inversion probes to analyze SNPs at >220,000 loci, as described previously.(4-6) Data generated by Affymetrix platform (probe signal intensity and genome location) were analyzed using Nexus Copy Number v5.1 software (BioDiscovery, El Segunda, CA).

Array comparative genomic hybridization (aCGH)

Array comparative genomic hybridization (aCGH) was performed from FFPE tissue blocks in 3 cases (#1, #2 and #10). A microarray: A CytoChip Focus Constitutional (BlueGnome Ltd, Cambridge, UK) was used for analysis, as previously described.(7) CytoChip Focus Constitutional uses BAC technology and covers 143 regions of known significance with 1 Mb spacing across a genome. Probes are spotted in triplicates. First, 400 ng of gDNA was labeled using the Fluorescent Labeling System (BlueGnome Ltd, Cambridge, UK). The procedure included Cy3 labeling of a test sample and Cy5 labeling of a reference sample. Commercially available reference of opposite sex was used in cases where no reference sample was available (MegaPool Reference DNA Male or MegaPool Reference DNA Female, Kreatech Diagnostics, Amsterdam, Netherlands). The labeled reference as well as the test sample were mixed, dried and hybridized overnight at 47 °C using ArrayIt hybridization cassettes (Arrayit Corporation, California, U.S.A.). Posthybridization washing was done using SSC buffers with increasing stringency. Dried microarrays were scanned with InnoScan 900 (Innopsys, France) at resolution 5 μm. Image and Data analysis: Scanned images were analyzed and quantified by BlueFuse Multi software (BlueGnome Ltd, Cambridge, UK). BlueFuse Multi uses Bayesian algorithms to generate intensity values for each Cy5 and Cy3 labeled spot on the array according an appropriate .gal file. The reported changes were browsed and interpreted using BlueFuse Multi as well. Cut off values were set to log 2 ratio to -0.193 for loss and 0.170 for gain.

Results

Clinical features

The clinicopathologic features and the follow-up data are shown in Table 1. All 16 renal tumors were identified in females, demonstrating no clinical features of TSC. One patient (#12) had a sister with a Birt–Hogg–Dubé syndrome, but tested negative for *folliculin (FLCN)* gene mutation. Mean patient age was 57 years (range, 31-75y). A single tumor was identified in each affected kidney and no multifocality was found. Ten patients had partial nephrectomy and 6 had radical nephrectomy. There was no predilection for laterality (left kidney 7; right kidney 9). Thirteen of 16 cases (81%) were stage pT1 (pT1a in 9, pT1b in 4); 2 were pT2 (pT2a in 1and pT2b in 2) and 1 was pT3a.

Follow-up was available for 14 of 16 patients. Thirteen of 14 patients were alive and without evidence of disease progression, after a follow-up ranging from 2 to 138 months (mean: 53 mo; median: 37.5 mo); 1 patient died of other causes after 14 months.

Pathologic findings

Macroscopic findings

Grossly, the tumors were yellow-gray to tan and the majority (12 of 16) showed a solid and cystic appearance, typically exhibiting a well-delineated mass with large macrocystic spaces, variable in size, and interspersed with solid nodules, as illustrated in Figure 1A. In some areas the cysts were separated by very thin cellular septa. The greatest tumor dimension was on average 50 mm (median, 38.5 mm; range 15-135 mm); however, the majority of tumors (10) measured up to 50 mm and only 2 exceeded 100 mm. The 4 cases that were exclusively solid, were smaller and measured from 15 to 33 mm in greatest dimension.

Microscopic findings

On microscopy, the tumors showed variably sized solid nests and confluent sheets, typically admixed with large macrocysts, showing variably thick septa composed of eosinophilic cells (Figure 1B). A well-formed capsule was absent at the tumor periphery. The cysts varied in size, and were lined by cells showing hobnail arrangement with voluminous eosinophilic cytoplasm (Figure 1C). Focally, there were areas with microcystic appearance with smaller cysts set within larger nodules composed of eosinophilic cells (Figure 1D). In some tumors, the septa of the cysts were compressed between the solid nodules and were more difficult to appreciate (Figure 1E). Four smaller tumors showed exclusively solid growth (Figure 1F).

The neoplastic cells had abundant eosinophilic cytoplasm and showed diffuse or tightly compact acinar or nested growth, and were typically admixed with small aggregates of histocytes and lymphocytes (Figure 2A-B). The cells had round to oval nuclei with focally prominent nucleoli (ISUP nucleolar grade 3). However, some cell variation was commonly present. Scattered cells had a peripheral rim of finely vacuolated or flocculent clear cytoplasm, focally showing marked size variation, variably coarse chromatin, and prominent nucleoli. Multinucleated cells were also common, focally forming clusters (Figure 2C). Within the solid foci, there were areas where the cells had less cytoplasm, imparting a more monotonous and basophilic appearance (Figure 2D). In examples with larger foci of basaloid cells, a nested or insular arrangement was seen (Figure 2E). One of the very characteristic features was the presence of fine or coarse cytoplasmic stippling (basophilic to purple cytoplasmic granules) (Figure 2F). Although focal, rare cells also showed densely eosinophilic to purple cytoplasmic globules, surrounded by a delicate clear rim

(Figure 2F inset). The cell morphology was identical in cases demonstrating only solid pattern, without the cystic component.

In some cases, although a typical morphology was present in most of the sections, there were focal areas showing unusual features, such as clear cell change (Figure 3A), focal papillary arrangement (Figure 3B), tubular architecture (Figure 3C), marked intracytoplasmic vacuolization (Figure 3D) and vaguely chromophobe-like areas (Figure 3E). Rare calcifications, including psammoma bodies, were also noted, usually adjacent to the cystic lumina (Figure 3F).

Immunohistochemistry

The complete immunohistochemistry (IHC) results are shown in Table 2. The neoplastic cells typically demonstrated nuclear PAX-8 reactivity (100%) (Figure 4A), patchy cytoplasmic AMACR staining (Figure 4B), and usually diffuse (or less often focal) cytokeratin (CK) 20 reactivity (Figures 4C and 4D), but showed only minimal focal or no staining for cytokeratin 7 (Figure 4E) or CD117 (Figure 4F). Of note, the 2 cases that were considered CK20 negative did show rare isolated positive cells. EMA was either negative or focally positive and cytokeratins (AE1/AE3 and CK8/18) were positive or focally positive in great majority of cases. Vimentin was positive in 10/13 cases, CD10 was diffusely or focally positive in 10/13 cases, while CA9 was positive in 2/10 cases (cytoplasmic only). Tuberin was retained, while Hamartin was lost in all tested cases (10/10). The staining was also performed for several additional antibodies, but due to limited number of evaluated cases, they are not included in Table 2. The results for the additional antibodies are as follows: HMB45/Melan A - negative in 6/6; TFE-3 - negative in 4/4 (1 also confirmed by FISH); CK5/6 - negative in 7/8; SDHA and SDHB - positive cytoplasmic

staining in 2/2; ER/PR - both focally positive in 2/4; and Ki67 - reactive in <1% of cells in 5/5 cases.

Electron microscopy

The tissue was partly damaged by fixation and deparaffinization. Ultrastructural analysis however revealed polygonal cells organized in solid nests and tightly packed acinar structures with focally visible lumina (Figure 5A-B). Rudimentary intercellular junctions were present as well as relatively scarce microvilli on the luminal surface (Figure 5B). Most of the cells had oval nuclei with shallow invaginations and some of them also had one prominent nucleolus (Figure 5C). Although cytoplasmic organelles were poorly preserved, abundant rough endoplasmic reticulum, accompanied by granular material, was visible in the majority of neoplastic cells (Figure 5C-D). Larger amounts of glycogen particles, lipid droplets or complex vesicles were not found.

Molecular karyotyping

Molecular karyotyping profiles were successfully established for the 3 evaluated cases across the whole genome and are illustrated in Figure 6 A. Loss of heterozygosity (LOH) was found for all three cases at 16p11.2 –1 (22 genes) and at Xq11.1-12 LOH (20 genes). Cases #8 and #13 also revealed LOH on 11p11.2-1 (10 genes).

In particular, cases #2 and #8 revealed similar molecular alterations. Copy number (CN) gains were found at 1p13.3, 7p22.3 – 7q36.3 (nearly whole chromosome), 7p11.2 (high CN gain), 10q23.31, 13q14.2, and 16p13.3 – 16q24.3 (nearly whole chromosome). CN losses were found at 19p13.2, 19q13.2, Xp22.32, Xp11.2 – Xp11.23, Xp11.23 – Xp11.21, Xq13.2 –Xq13.3, and at

Xq23 – Yp11.32 (end of X telomere).

Array comparative genomic hybridization (aCGH)

aCGH was successfully carried out only in 1 (case #1) of the 3 evaluated cases (#1, #2 and #10). In this case, a gain of chromosome 16 was revealed, as illustrated in Figure 6B. The status of the remaining chromosomes was normal.

Discussion

We propose that the renal neoplasm described herein as "eosinophilic, solid, and cystic renal cell carcinoma" (ESC RCC) is a distinct subtype of renal epithelial neoplasm. The key features of ESC RCC are summarized in Table 3. In this study, it was found only in female patients and showed consistent gross and microscopic features, frequent CK20 reactivity, gain of chromosome 16, and an indolent clinical behaviour. While these ESC RCCs are virtually identical to the neoplasms previously documented in a subset of TSC patients,(1, 2) none of these current patients had any clinical or pathologic signs of TSC. The true incidence of ESC RCC is difficult to estimate, but the fact that we were able to identify only 1 to 2 cases in the majority of participating institutions with large uropathology practices, indicates that it is indeed very rare.

Two recent studies documented renal neoplasms showing identical morphology to those presented in this current study, but in association with TSC.(1, 2) We first learned of this histologic pattern through the published case study of Schreiner et al describing a 43-year-old

man with TSC and bilateral renal lesions, including multiple minute angiomyolipomas, cortical cysts, and 4 separate RCCs of unclassified type.(1) The carcinomas shared distinctive morphological features, including sheet-like, glandular, trabecular, or cystic architecture and abundant granular eosinophilic cytoplasm. One of the 4 tumors, labelled "RT1" (morphology illustrated in their Figure 1, B-D (1)), in our view, is identical to the cases described herein. It demonstrated solid areas composed of eosinophilic epithelioid cells arranged in acinar formation. In many areas, higher grade nuclei were present (Fuhrman grade 3) and multinucleated cells were seen in clusters, as seen in the cases presented in the current study.

Prompted by an index case seen in consultation, which demonstrated similar morphology to renal neoplasm "RT1" described by Schreiner et al, Guo et al collected a series of 57 separate renal cell carcinomas (RCC) in 18 patients with TSC and described three distinct morphologies.(2) They documented 6 RCCs (11% of all evaluated tumors), demonstrating "granular eosinophilic-macrocystic morphology', which were essentially identical to the tumors described in the present study. This patient group actually represented 33% (6/18) of all included TSC patients, and all 6 were females, with a single tumor per kidney, as in the present study. Of the remaining cases, 17 RCCs (30%) had features similar to the tumors previously described as "renal angiomyoadenomatous tumor" or "RCC with smooth muscle stroma", while 34 RCCs (59%) showed features similar to chromophobe RCC (or hybrid oncocytic tumors); multifocality was frequent in these two groups. Several of the co-authors of the current study participated in the Guo et al study (2), and had an opportunity to evaluate and compare the 6 tumors with "eosinophilic-macrocystic morphology" (illustrated in Figure 3 by Guo et al (2)), to the ones included in this study. Based on the morphologic features and the IHC profile, we concluded that

both groups, those associated with and without TSC, are pathologically identical. Moreover, all 6 cases associated with TSC showed similar IHC profile: PAX8 positive, CK7 only focally positive; negative for CA9, CD117 and HMB45. Unfortunately, CK20 reactivity, one of the key IHC findings in the present study, was not evaluated by Guo et al.(2) We have retrospectively evaluated 2 of the originally reported cases and both show strong patchy cytoplasmic immunoreactivity for CK20 (unpublished data), similar to the sporadic cases presented herein. Although CK20 is not routinely investigated or included in an immunopanel to evaluate renal tumors, we found it to be quite helpful in supporting the diagnosis of this tumor, as 14 of 16 (88%) cases in this series showed either diffuse (69%) or focal (19%) cytoplasmic reactivity for CK20. Admittedly, this finding was completely serendipitous, as the stain had been performed at the time of original evaluation on the archived index case. In our experience, CK20 is typically negative in the common renal neoplasms that may be considered in the differential diagnosis of ESC RCC.

In addition to the common association with AML, there are multiple additional reports of renal neoplasms with variable morphologies seen in association with TSC (mostly as case reports or small series), including clear cell, papillary, chromophobe and unclassified RCC, as well as cases labelled “oncocytoma”.(8-13) We could not find any tumors with morphologic features similar to the ones described herein in these previous studies.(8-13) Another recent series of RCCs in TSC (14) did not document any tumors with this unique eosinophilic and cystic morphology.

TSC results from mutations in 1 of 2 interacting gene products, hamartin, associated with *TSC1* (located on chromosome 9q34) and tuberin, associated with *TSC2* (located on chromosome

16p13). Although it is known that they are expressed and co-localized in most normal human tissues, including the proximal and distal renal tubules and collecting ducts, there are some differences in expression within different types of renal tubules.(15) However, the expression of hamartin and tuberin has not been well studied in renal tumors and they are not used as part of the routine IHC evaluation in this setting. Prompted by the previous association of these gene products with TSC, we tested 10 of 16 available cases by IHC, and found that tuberin was retained, while hamartin was lost in all tested cases. The significance of this finding is uncertain at this time. Of note, we have also found that tuberin was positive in 4/4 of ESC RCC associated with TSC, while hamartin was negative in 3/4 cases (1 was weak positive) (unpublished data). It is interesting to note that the aCGH showed a gain of chromosome 16 in case #1 and that molecular karyotyping of cases #2 and #8 also showed CN gain affecting nearly the whole chromosome 16 (16p13.3 – 16q24.3), which encompasses the tuberin encoding region Although the patients in this study had no clinical evidence of TSC, it is well known that TSC has a high de novo mutation rate, and such an event cannot be completely ruled out.(16) Although genetic testing for TSC was not done in the patients included in the study (which is a study limitation), even the molecular genetic testing for TSC, often done in specialized centers, appears to be complex and imperfect. For example, it was reported that 16.9% of patients who met the clinical criteria for TSC had no identified mutation by standard genotyping.(16) Additionaly, none of the patients in this study had any AMLs found in the adjacent renal parenchyma, which are invariably seen in patients with classic TSC.

The molecular karyotyping results, although available on only 3 of 16 cases, revealed a unique pattern of alterations. LOH at 16p and Xq11was found in all 3 evaluated cases; LOH at 11p was

found in 2 of 3 cases (#8 and #13). Cases #2 and #8, in particular, showed a distinct pattern of CN gains (1p, 7p, 10q, 13q, 16p and 16q) and CN losses (19p, 19q, Xp, and Xq). Similarly, aCGH showed a gain of chromosome 16. These results provide additional evidence supporting a distinct genetic profile in these neoplasms that is different from the well-characterized renal neoplasms with known recurrent genetic alterations.

The differential diagnosis of ESC RCC includes other renal tumors with eosinophilic cytoplasm, such as oncocytoma, eosinophilic variant of chromophobe RCC, SDH deficient RCC, MiT translocation type RCC, and epitheliod AML. Other more common RCCs, such as clear cell RCC, particularly of higher grade, and the solid variant of papillary RCC, primarily the oncocytic type, may also be considered in the differential. Some of these indeed may show a more cystic appearance (such as clear cell carcinoma), but the features of the ESC RCC, as described herein, are sufficiently distinct in our opinion, to distinguish them from the other renal tumors. Both oncocytoma and eosinophilic chromophobe RCC typically have a more uniform architecture, without a macrocystic component, and both also show more uniform cytology. While rare focal areas in ESC RCC did superficially resemble chromophobe RCC, well-developed perinuclear halos and more irregular nuclear membranes were not a prominent feature. Both oncocytoma and eosinophilic chromophobe RCC are also typically reactive for CD117 (C-kit), which was uniformly negative in ESC RCC. In addition to CK20, which should be negative in both oncocytoma and chromophobe RCC, CK7 is typically diffusely positive in chromophobe RCC, and either negative or only focally reactive in minority of ESC RCC, similar to oncocytoma. SDH deficient RCC, is a recently characterized, distinct and rare renal neoplasm, defined by loss of IHC staining for SDHB and germline mutations of the *SDH* genes.(17)

Although it may show focal microcystic changes, macrocysts were not documented. SDH deficient RCC typically exhibits uniform low-grade cytology, with cytoplasmic vacuoles, and eosinophilic or flocculent cytoplasm. Two cases in the present study (#1 and #2) were also tested and demonstrated positive IHC staining for SDHA and SDHB (SDHB is typically negative in SDH deficient RCC). Although rare examples of MiT translocation type RCC (most often Xp11) may show mostly eosinophilic morphology, they more often show clear cell morphology with cells exhibiting a voluminous cytoplasm, typically not seen in ESC RCC. MiT translocation type RCC also typically show papillary and nested architecture. TFE3 was also tested in 4 cases by IHC in this study and it was consistently negative (1 case also tested negative by FISH). Epithelioid AML is another relatively rare tumor, which despite the morphologic similarities with ESC RCC, in many cases demonstrates more prominent pleomorphism. More importantly, epithelioid AML does not label for cytokeratins, while it is positive for HMB45/Melan A, which is the opposite phenotype of ESC RCC. In addition, the demonstration of nuclear PAX-8 expression essentially excludes AML in our experience. Higher grade clear cell RCCs may also show eosinophilic morphology and macrocysts, but they typically have a delicate vascular pattern, which was not seen in ESC RCC. Clear cell RCC also does not label for CK20, but typically have strong membranous reactivity for CA9, opposite of the pattern seen in ESC RCC (CK20 positive, CA9 negative). Additionally, it is not entirely uncommon for the epithelial cyst lining in cystic areas of clear cell RCC to show strong immunoreactivity for CK7, another finding not seen in ESC RCC.(18) Although the oncocytic variant of papillary RCC typically demonstrates predominantly papillary growth, less frequent solid patterns are also well-described.(19) Papillary architecture was present only focally in 1 case of ESC RCC. Oncocytic papillary RCC also shows more uniform cytology, and typically has a CK7 positive, CK20

negative immunophentype. Finally, the cytoplasmic stippling, a characteristic feature of ESC RCC, to our knowledge, is not reported in any of the recognized renal neoplasms and none of the renal tumors listed in the differential have such a striking female predominance. The key features and the immunostains that can be used to distinguish ESC RCC from other renal tumors are shown in Table 4.

Although all tumors in this study with available clinical follow-up demonstrated an indolent clinical course, with no evidence of either recurrence or metastatic disease, the limited number of studied cases so far, precludes a definitive confirmation of its benign nature. Additional studies with longer follow-up would be needed to confirm their outcome over an extended clinical course. While the label "uncertain malignant potential" has also been used to designate tumors of controversial and debatable biologic nature, we decided to designate these tumors as "eosinophilic, solid and cystic RCC" (ESC RCC), in a descriptive manner, which, in our view adequately captures the tumor morphology. Other recently described specific subtypes of indolent renal neoplasia have followed the same approach with designation of renal cell carcinoma and an accompanying descriptive name (e.g. mucinous tubular and spindle cell RCC, clear cell papillary RCC, or tubulocystic RCC).(3) We considered using the descriptor "macrocystic" instead of "cystic", but favoured "cystic", because it is a more general term that incorporates both the macro and the microcystic component. Should additional information become available in the future to better characterize the nature of this tumor, appropriate adjustment could be made regarding the diagnostic terminology.

In conclusion, ESC RCC appears to be a unique renal neoplasm that is predominantly found in females, and shows distinct morphologic features, frequent CK20 reactivity, gain of chromosome 16, and indolent clinical behaviour. They appear histologically identical to a subset of renal neoplasms seen in TSC patients, but in this study, they were found in a sporadic setting. Awareness of the clinical, morphologic and immunophenotypic features of this novel renal neoplasm will increase its recognition and will allow surgical pathologists to re-evaluate similar renal tumors, previously considered "unclassified".

References

1. Schreiner A, Daneshmand S, Bayne A, et al. Distinctive morphology of renal cell carcinomas in tuberous sclerosis. Int J Surg Pathol. 2010;18:409-418.

2. Guo J, Tretiakova MS, Troxell ML, et al. Tuberous Sclerosis-associated Renal Cell Carcinoma: A Clinicopathologic Study of 57 Separate Carcinomas in 18 Patients. Am J Surg Pathol. 2014;38:1457-1467.

3. Srigley JR, Delahunt B, Eble JN, et al. The International Society of Urological Pathology (ISUP) Vancouver Classification of Renal Neoplasia. Am J Surg Pathol. 2013;37:1469-1489.

4. Wang Y, Carlton VE, Karlin-Neumann G, et al. High quality copy number and genotype data from FFPE samples using Molecular Inversion Probe (MIP) microarrays. BMC Med Genomics. 2009;2:8.

5. Wang Y, Moorhead M, Karlin-Neumann G, et al. Allele quantification using molecular inversion probes (MIP). Nucleic Acids Res. 2005;33(21):e183.

6. Wang Y, Moorhead M, Karlin-Neumann G, et al. Analysis of molecular inversion probe performance for allele copy number determination. Genome Biol. 2007;8:R246.

7. Petersson F, Vanecek T, Michal M, et al. A distinctive translocation carcinoma of the kidney; "rosette forming," t(6;11), HMB45-positive renal tumor: a histomorphologic, immunohistochemical, ultrastructural, and molecular genetic study of 4 cases. Hum Pathol. 2012;43:726-736.

8. Bjornsson J, Short MP, Kwiatkowski DJ, et al. Tuberous sclerosis-associated renal cell carcinoma. Clinical, pathological, and genetic features. Am J Pathol. 1996;149:1201-1208.

9. Kang SG, Ko YH, Kang SH, et al. Two different renal cell carcinomas and multiple angiomyolipomas in a patient with tuberous sclerosis. Korean J Urol. 2010;51:729-732.

10. Jimenez RE, Eble JN, Reuter VE, et al. Concurrent angiomyolipoma and renal cell neoplasia: a study of 36 cases. Mod Pathol. 2001;14:157-63.

11. Paul E, Thiele EA, Shailam R, et al. Case records of the Massachusetts General Hospital. Case 26-2011. A 7-year-old boy with a complex cyst in the kidney. N Engl J Med. 2011;365:743-751.

12. Kubo M, Iwashita K, Oyachi N, et al. Two different types of infantile renal cell carcinomas associated with tuberous sclerosis. J Pediatr Surg. 2011;46:E37-41.

13. Al-Saleem T, Wessner LL, Scheithauer BW, et al. Malignant tumors of the kidney, brain, and soft tissues in children and young adults with the tuberous sclerosis complex. Cancer. 1998;83:2208-2216.

14. Yang P, Cornejo KM, Sadow PM, et al. Renal cell carcinoma in tuberous sclerosis complex. Am J Surg Pathol. 2014;38:895-909.

15. Johnson MW, Kerfoot C, Bushnell T, et al. Hamartin and tuberin expression in human tissues. Mod Pathol. 2001;14:202-210.

16. Rakowski SK, Winterkorn EB, Paul E, et al. Renal manifestations of tuberous sclerosis complex: Incidence, prognosis, and predictive factors. Kidney Int. 2006;70:1777-1782.

17. Gill AJ, Hes O, Papathomas T, et al. Succinate Dehydrogenase (SDH)-deficient Renal Carcinoma: A Morphologically Distinct Entity: A Clinicopathologic Series of 36 Tumors From 27 Patients. Am J Surg Pathol. 2014;38:1588-1602.

18. Williamson SR, Halat S, Eble JN, et al. Multilocular cystic renal cell carcinoma: similarities and differences in immunoprofile compared with clear cell renal cell carcinoma. Am J Surg Pathol. 2012;36:1425-1433.

19. Renshaw AA, Zhang H, Corless CL, et al. Solid variants of papillary (chromophil) renal cell carcinoma: clinicopathologic and genetic features. Am J Surg Pathol. 1997;21:1203-1209.

Figure legends:

Figure 1: Typical architectural patterns in eosinophilic, solid and cystic renal cell carcinoma. A) The macroscopic features include a well-delineated mass with large macrocystic spaces interspersed with tan solid nodules. B) Histologically, the dilated macrocystic spaces are lined by neoplastic cells characterized by voluminous eosinophilic cytoplasm and C) a prominent hobnail arrangement. D) Some foci have a microcystic appearance with smaller cysts set within large nodules of the eosinophilic cells. E) In some tumors, the septa of the cysts (arrows) are compressed between solid nodules and are more difficult to appreciate, while F) rare examples have a completely solid growth.

Figure 2: Typical cytologic features in eosinophilic solid and cystic renal cell carcinoma. A) The neoplastic cells have abundant eosinophilic cytoplasm and admixed aggregates of histocytes and lymphocytes are invariably present. B) The neoplastic cells had tightly compact acinar or nested growth. C) Multinucleated cells are also common. D) Within the solid foci, some cells have less cytoplasm imparting a more monotonous and basophilic appearance (arrows). E) In examples with large foci of basaloid cells, a nested/insular arrangement may be seen. F) The cytoplasm characteristically shows fine (small arrow) or coarse stippling (large arrow). Rarely, there were cells with larger, eosinophilic to purple cytoplasmic globules, surrounded by a delicate clear rim (inset).

Figure 3: Unusual features in eosinophilic, solid and cystic renal cell carcinoma include: A) focal clear cell change; B) focal papillary change (arrows show residual septa of more typical macrocysts); C) tubular architecture; D) marked intracytoplasmic vacuolization; E) chromophobe–like areas; and F) focal calcifications, typically adjacent to the cysts.

Figure 4: Typical immunophenotypic features of eosinophilic, solid and cystic renal cell carcinoma: A) Nuclear PAX-8 reactivity; B) Patchy cytoplasmic AMACR staining; C) Diffuse or D) patchy cytokeratin 20 immunoreactivity; E) No staining with cytokeratin 7 or F) CD117.

Figure 5: Electron micrographs of neoplastic cells of eosinophilic, solid and cystic renal cell carcinoma. A) Polygonal cells arranged in solid nests. B) Structures with focal lumina and visible short microvilli. C-D) Abundant rough endoplasmic reticulum accompanied by granular material was visible in the majority of neoplastic cells. The nuclei were oval with shallow invaginations and some of them also had one prominent nucleolus (C, upper right corner).

Figure 6: A) Molecular karyotyping profiles showing copy number (CN) gains and losses from 3 cases (#2, #8 and #13) (blue denotes CN gains; red denotes CN loses); B) aCGH result from case #1, showing a gain of chromosome 16.

Table 1: Clinicopathologic features and follow-up of eosinophilic, solid and cystic renal cell carcinoma (ESC RCC)

Patient	Location	Age (years) / Gender	Tumor size (mm)	Surgery (Type)	Gross	Stage	ISUP grade	Status	Follow-up (months)
1	R	69 F	18	Partial	Tan, solid and cystic	pT1a	3	ANED	138
2	L	74 F	53	Radical	Tan, solid and cystic	pT1b	3	DOC	14
3	R	54 F	44	Partial	Tan, solid and cystic	pT1a	3	ANED	6
4	R	49 F	15	Partial	Tan, solid	pT1a	3	NA	NA
5	L	75 F	58	Partial	Tan, solid and cystic	pT1b	3	ANED	15
6	L	63 F	19	Partial	Brown-yellow	pT1a	3	ANED	39
7	R	56 F	65	Partial	Tan, solid and cystic	pT1b	3	ANED	36
8	R	47 F	30	Radical	Tan, solid	pT1a	3	ANED	8
9	L	66 F	80	Radical	NA	pT2a	3	ANED	60
10	R	66 F	135	Radical	NA	pT3a	3	ANED	130
11	R	50 F	20	Partial	Tan, solid and cystic	pT1a	3	ANED	32
12*	L	44 F	45	Partial	Tan, cystic and solid	pT1b	3	ANED	53
13	L	45 F	33	Radical	Tan, solid	pT1a	3	NA	NA
14	L	31 F	130	Radical	NA	pT2b	3	ANED	144
15	R	53 F	30	Partial	NA	pT1a	3	ANED	75
16	R	69 F	18	Partial	Tan solid	pT1a	3	ANED	2

ANED = alive no evidence of disease; NA = not available; DOC = died of other causes

* Sister with Birt-Hogg-Dubé syndrome; patient tested negative for FLCN (folliculin) mutation

Table 2. Immunohistochemistry results for eosinophilic, solid and cystic renal cell carcinoma (ESC RCC)

Patient	Pax8	AMACR	CD10	CD117	EMA	CK7	CK20	CA9	AE1/AE3	CK8/18	Vimentin	Hamartin	Tuberin
1	+	+/-	-	-	+/-	-	+	NA	+/-	+	-	-	+
2	+	+	+	-	+/-	-	+/-	NA	+/-	+	+	-	+
3	+	-	-	NA	NA	+/-	+	+	-	+	-	NA	NA
4	NA	+/-	NA	NA	-	-	+	-	-	+	+/-	-	+
5	+	NA	NA	NA	NA	-	+	NA	NA	NA	NA	-	+
6	+	+/-	NA	NA	NA	+/-	+	-	NA	NA	NA	-	+
7	+	+/-	+	-	-	-	+/-	+	+/-	+	-	-	+
8	+	+/-	+/-	-	-	-	+	-	+/-	+	+	-	+
9	+	-	+	-	-	-	+	-	-	+/-	+	NA	NA
10	+	-	+	-	+/-	-	-	-	+/-	+	+	NA	NA
11	+	+/-	-	+/-	-	-	-	-	+/-	+/-	+	-	+/-
12	+	+/-	+/-	-	+/-	+/-	+	NA	+/-	+/-	+	-	+
13	+	+/-	+/-	-	-	-	+	-	+	+	+	-	+
14	+	+	+/-	-	-	-	+/-	NA	+	+	+	NA	NA
15	+	+/-	+	-	-	+/-	+	-	+	+	+	NA	NA
16	+	+	+/-	-	NA	-	+	NA	NA	NA	NA	NA	NA
Percent pos*	100%	80%	77%	8%	33%	25%	88%	20%	77%	100%	77%	0%	100%

‘+ ‘= positive, '-' = negative, '+/-' = focal; 'NA' = not available

* Percent positive includes both focal and diffuse positive cases, excluding cases with unavailable result

Table 3: Summary of the key features of eosinophilic, solid and cystic renal cell carcinoma (ESC RCC)

Clinical	Females only, usually low stage, good prognosis
Gross	Solid and cystic or solid (minority), yellow-gray, single tumors
Light microscopy	Architecture: Solid and cystic, diffuse or tightly compact acinar or nested growth, capsule absent Cytology: Eosinophilic voluminous cytoplasm with stippling, round to oval nuclei, prominent nucleoli (ISUP nucleolar grade 3). Scattered foamy histyocytes, lymphocytes and multinucleated cells. Hobnail cells line the cysts.
Immunohistochemistry	Positive: PAX-8, CK20, Vimentin, AMACR (+/-), CD10 (+/-), Tuberin Negative: CA9, CD117, CK7, HMB-45, Hamartin
Electron microscopy	Abundant rough endoplasmic reticulum
Molecular karyotype	LOH: 16p and Xq (3/3 cases); 11p (2/3 cases) CN gains: 1p, 7p, 10q, 13q, 16p (2/3 cases) CN losses: 19p, 19q, Xp, Xq (2/3 cases)
aCGH	gain of Chr 16

LOH = loss of heterozigosity; CN = copy number

Table 4: Key features and immunostains helpful in distinguishing eosinophilic, solid and cystic renal cell carcinoma (ESC RCC) from other renal tumors

Diagnosis	**Key distinguishing features**	**Immunohistochemistry**
Eosinophilic, solid and cystic RCC	Only females, solid and cystic growth, voluminous eosinophilic cytoplasm, cytoplasmic stippling, usually low stage	CK20+, CK7-/+, CD117-, PAX8+, CA9-, HMB45-, PanCK+
Chromophobe RCC, eosinophilic	Solid and uniform architecture, irregular nuclear membranes, perinuclear halos	CD117+, CK7+, CK20-
Oncocytoma	Uniform cytology, lacks macrocysts	CD117+, CK7 -/+, CK20-
Epithelioid angiomyolipoma	Epithelioid cells which may be pleomorphic, lacks macrocysts	PAX8-, HMB45+, PanCK-, CK7-, CK20-
Papillary RCC, oncocytic	Papillary formations (at least focal), uniform cytology	CK7+, CK20-
Clear cell RCC, eosinophilic morphology	Focal clear cell areas, delicate vasculature, may contain macrocysts	CA9+, CK20-
MiT translocation RCC	Large cells with clear (or eosinophilic) morphology, focal papillary and nested growth, lack cysts (usually)	TFE3+, TFEB+, HMB45+
SDH-deficient RCC	Lacks macrocysts, uniform low-grade oncocytic cells with flocculent cytoplasms, cytoplasmic vacuoles	CD117-, SDHB-, SDHA+, CK7-, CK20-

Figure 1
Click here to download high resolution image

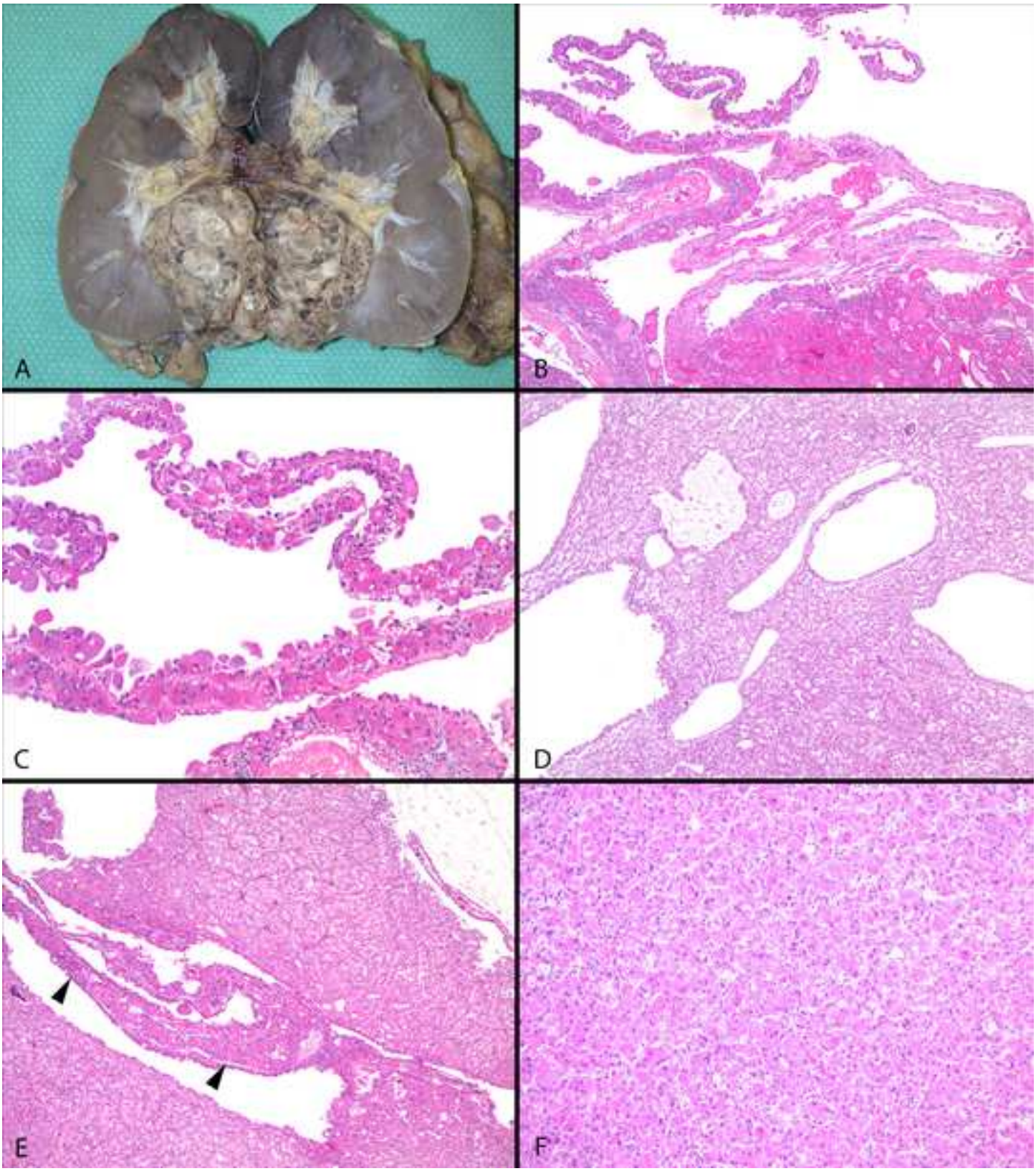

Figure 2
Click here to download high resolution image

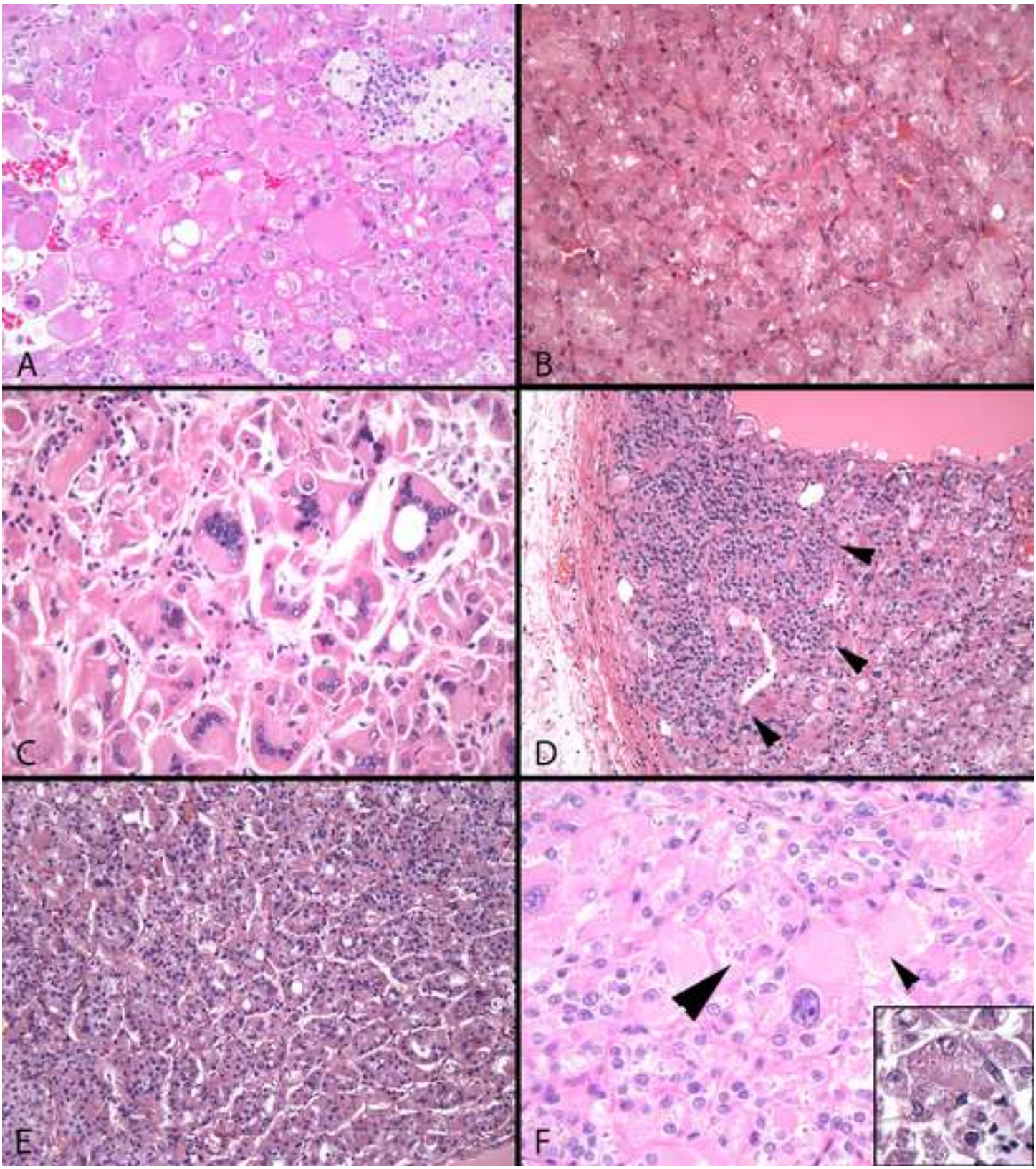

Figure 3
Click here to download high resolution image

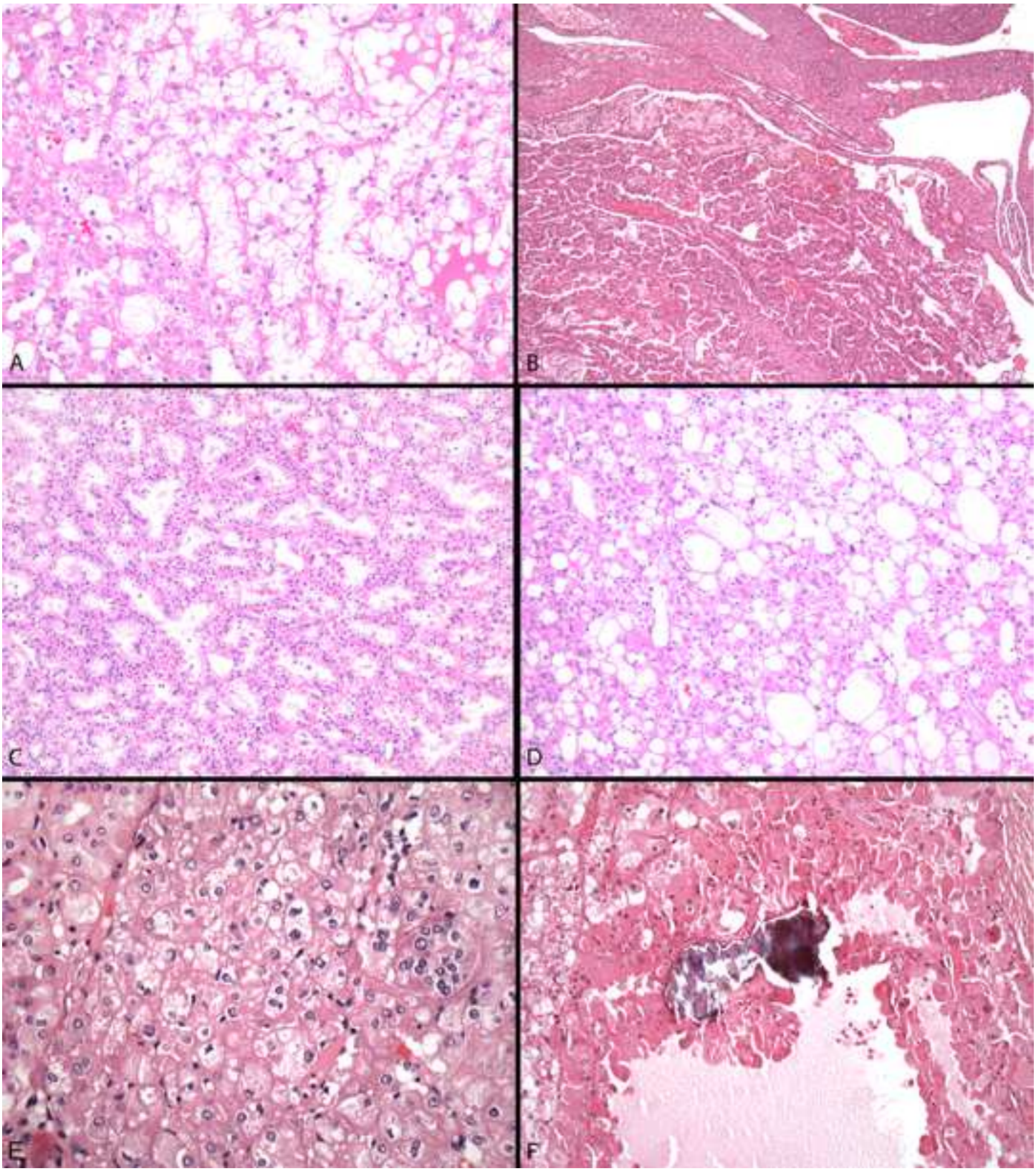

Figure 4
Click here to download high resolution image

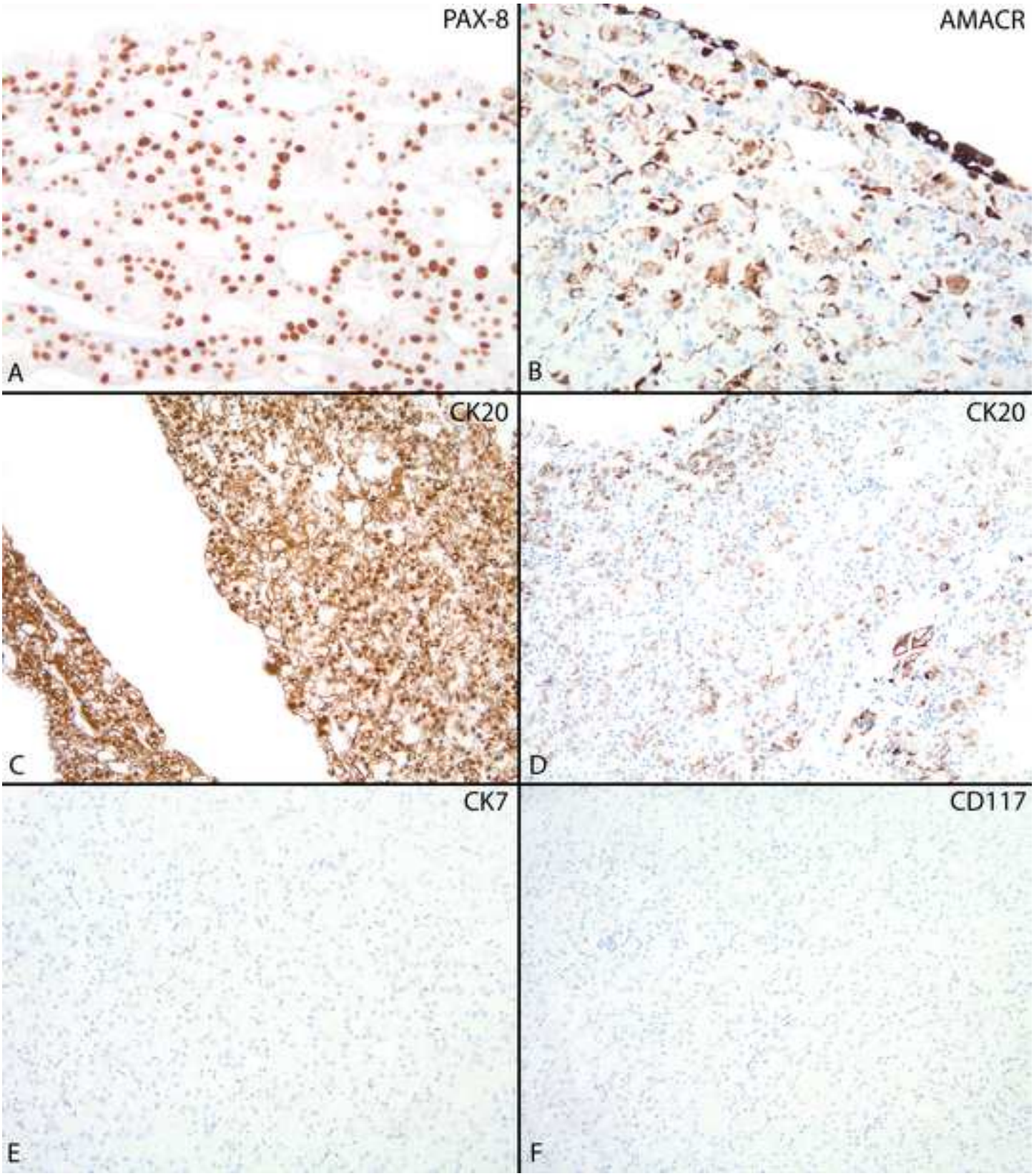

Figure 5
Click here to download high resolution image

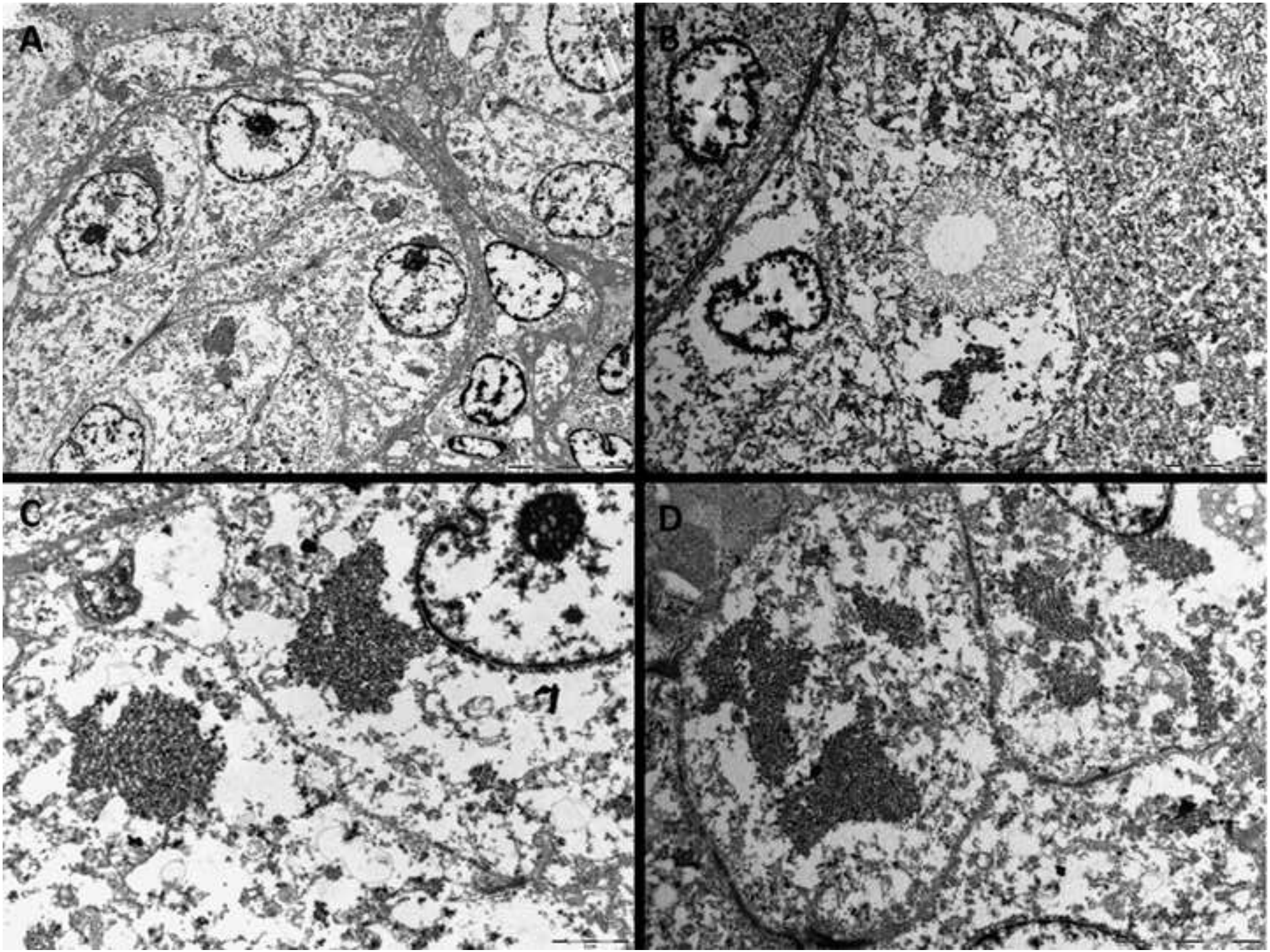

Figure 6A

A.

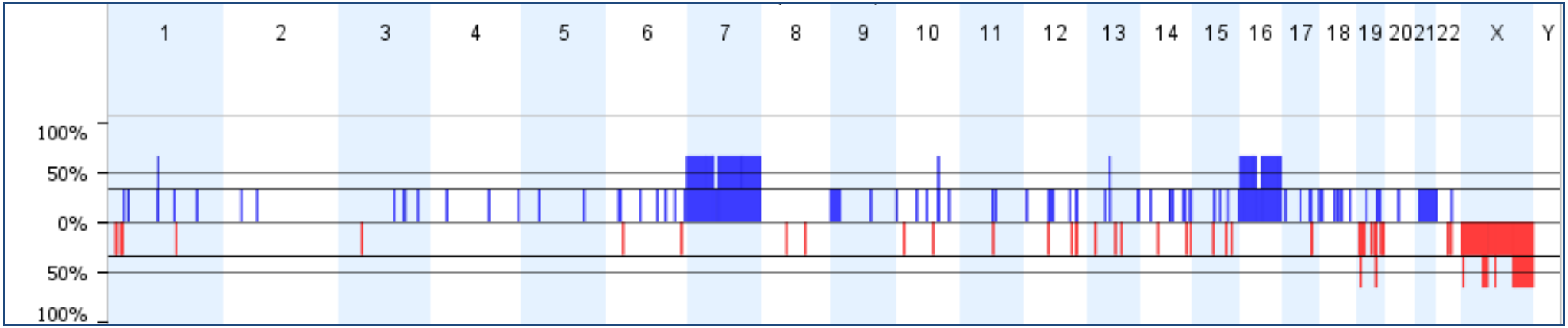

Figure 6B

Click here to download high resolution image

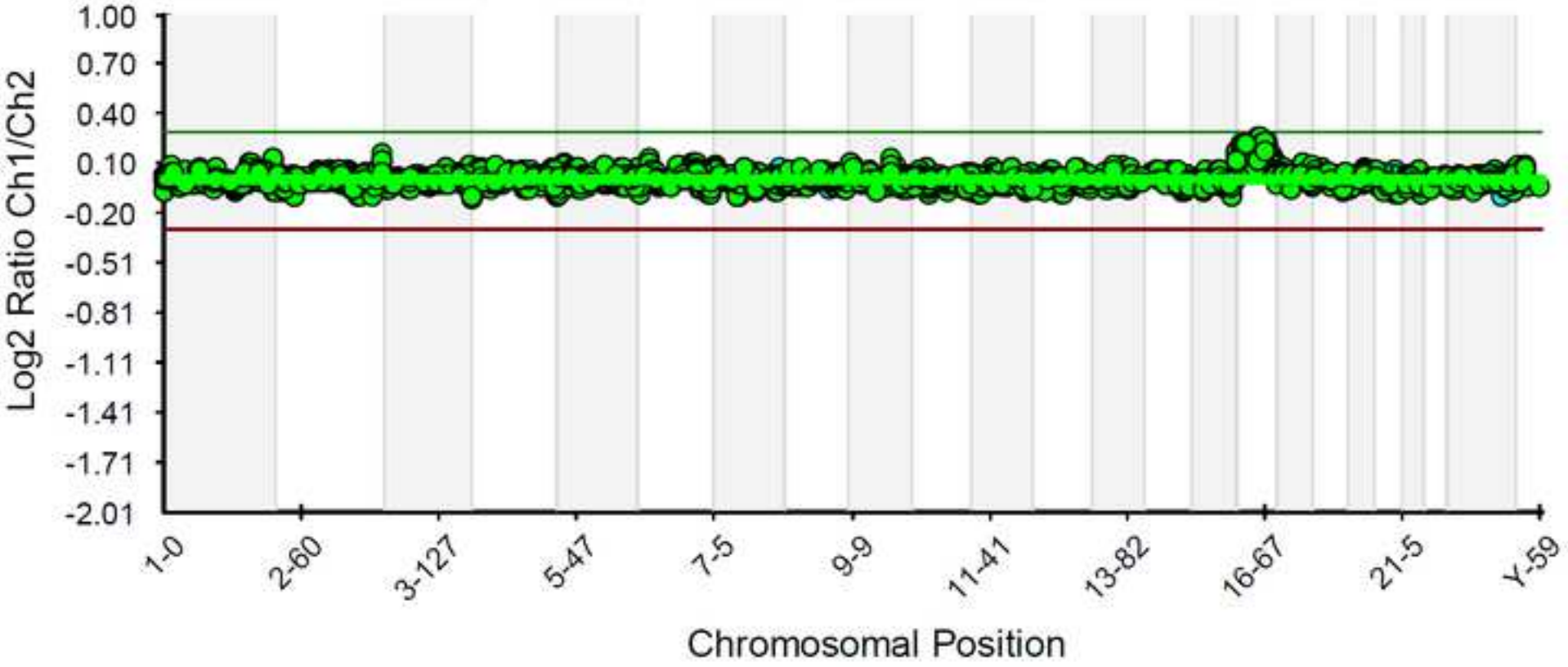

LWW Copyright Transfer and Disclosure Form
Click here to download LWW Copyright Transfer and Disclosure Form: copyrightTransfer_Trpkov_ESC RCC.pdf